JAST, Vol. 13, No. 1, pp. 48-56

Science Article

Simulation and Examination of Flow Characteristics of the Butterfly Valve

Fathollah Ommi[1], Hamidreza Khodayari[2], Zoheir Saboohi[3]

1-2. Faculty of Mechanical Engineering, Tarbiat Modares University
3. Aerospace Research Institute, Ministry of Science, Research, and Technology
*PO Box 111-14115, Nasr Bridge, Jalal Al-Ahmad, Tehran

Email: ***ommi@modares.ac.ir**

Butterfly valves as control valves are used when a small pressure drop is required in the valve. The results of numerical studies of solving the incompressible flow equations around the butterfly valve in three dimensions are presented in this paper. ANSYS CFX commercial software is used to solve the flow equations. The ε-k turbulence model is used to simulate flow disturbances. Velocity, pressure distribution, kinetic energy, and turbulence intensity profiles are the factors that provide flow characteristics. The position of the disk at the opening angles of 0°, 15°, 30°, 45°, 60°, and 75° as well as the inlet velocities of 1, 2, and 3 m/s have been investigated. Torque and valve performance factors such as flow coefficient and Hydrodynamics torque coefficient have been calculated for these different opening angles. The results of this simulation have been compared with the available experimental results for validation. The results show that the pressure drop across the valve, the flow coefficient, and the hydrodynamic torque coefficient depend on the opening angle. As the opening angle increases, the flow coefficient and the hydrodynamic torque coefficient decrease, and the torque and pressure drop increase across the valve. Flow separation has also been investigated at the mentioned opening angles.

Keywords: *Butterfly Valve, Hydrodynamic Torque Coefficient, Flow Coefficient, Turbulence*

Introduction

A butterfly valve controls flow and is widely used in various industries such as oil and gas transmission lines, water pipelines, and power plants. This type of valve has many applications due to its simple assembly, low cost, low time needed for opening and closing, and low pressure drop in the fully open state. As is evident in figure 1, the main components of this valve include the disc, shaft, and body of the valve. The shaft is located at the center of the disk rotation, which changes its position from parallel to the flow to perpendicular. Preliminary studies on butterfly valves include experimental and analytical studies. Sarpkaya (1) theoretically predicted a butterfly valve's cavitation and torque characteristics. Morris and Dalton experimentally studied the

1 Professor (corresponding author)
2 PhD student
3 Assistant professor

Received: 05 March 2020
Accepted: 04 May 2020

aerodynamic torque characteristics of a butterfly valve using two-dimensional and three-dimensional models.

Figure 1. Butterfly valve

This study shows the effect of the flow separation phenomenon on aerodynamic characteristics of butterfly valve torque. Kimura theoretically studied the pressure drop and cavitation characteristics of a butterfly valve. The relationships between the obtained theoretical pressure drop coefficients and the drop coefficient and the critical cavitation number were studied. Ogawa and Kimura [4] theoretically conducted studies to predict the hydrodynamic torque characteristics of a butterfly valve. They obtained the relations of torque characteristics using theoretical studies and considering the empirical information of torque measurements. Due to the rapid expansion of computational power and numerical methods, many researchers have used numerical methods and computational fluid dynamics to study flow phenomena in a butterfly valve. Using numerical methods, Kim and Huang [5] studied the incompressible flow around the butterfly valve disk in three dimensions. Their studies showed the pressure distribution and flow velocity around the disk. Lin and Schohl [6] investigated the hydrodynamic forces on the semi-open disk using Fluent Commercial Software. Their results show the accuracy of the results obtained from computational fluid dynamics compared to experimental results to estimate the force and discharge coefficient. Song and Park [7] simulated a butterfly valve in an incompressible stream and at different opening angles in a three-dimensional state. The background flow and the values of pressure drop, flow coefficient, and hydrodynamic torque are calculated in the results obtained. Perma [8] numerically studied the geometry of a butterfly valve and its effects on valve performance in the fully open state. This paper aims to solve the flow equations around the circular disc of a butterfly valve at opening angles of 0˚, 15˚, 30˚, 45˚, 60˚, and 75˚ and inlet velocities of 1, 2, and 3 m/s in a three-dimensional state to investigate the flow behavior around the valve and predict the torque on the disk and valve performance factors using CFX commercial software.

Geometry and boundary conditions

In order to compare with Chaiworapuek's experimental results [9], the diameter of the circular disk of the butterfly valve is equal to 50 mm, and the diameter of the tube is 52 mm in our study. According to studies conducted by Huang and Kim, the upstream and downstream lengths of the butterfly valve disk should be at least 2 to 8 times the length of the disk in order to have fully expanded inlet and outlet flow. Therefore, in this paper, the upstream length of the disk is considered four times, and the downstream length is considered 12 times the length of the butterfly valve disk to reach accurate calculations. Figure 2 shows the geometry and dimensions of the butterfly valve to be simulated.

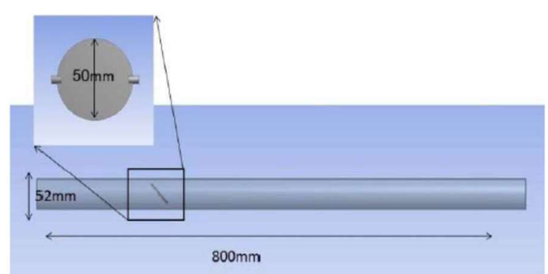

Figure 2. Geometry and dimensions of the butterfly valve

The boundary conditions used in this simulation are also shown in figure 3. The entry boundary condition is set at inlet velocities of 1, 2, and 3 m/s. The pressure at the outlet boundary condition is zero to determine the pressure difference and drop. The wall of the tube and the disc of the butterfly valve also have the boundary condition of the wall

without slipping. In this simulation, the physical properties of water as fluid are used. Half of the flow environment is modeled for simulation to reduce the solving time and consider symmetry in the problem.
Given the proper length at the inlet, the flow before the disk is uniform. The flow in the hydrodynamic state must be fully developed at the channel outlet.

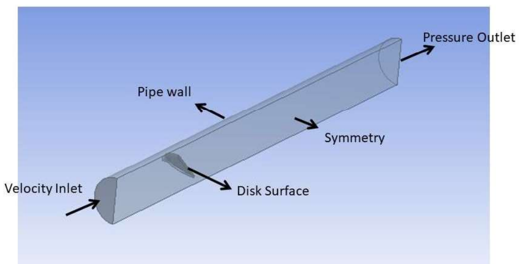

Figure 3. Boundary conditions for the computational environment

Computational network

The geometry of the problem with the dimensions mentioned in the previous section has been designed by Design-modeller software, and its computational network has been networked by ICEM-CFD software.
The multidimensional network is the primary model for CFD simulations in this study. The resulting multidimensional cells typically have 14 facets and provide a balanced solution in terms of computational cost. A significant advantage of the multidimensional mesh model compared to the quadrilateral mesh is its relatively easy and efficient production. Therefore, its computational cost is reduced. The prism model is used to produce the boundary cells along the wall. This layer of cells helps dissolve the boundary layer and improve the accuracy of flow resolution. The computational network has 325/150 cells.

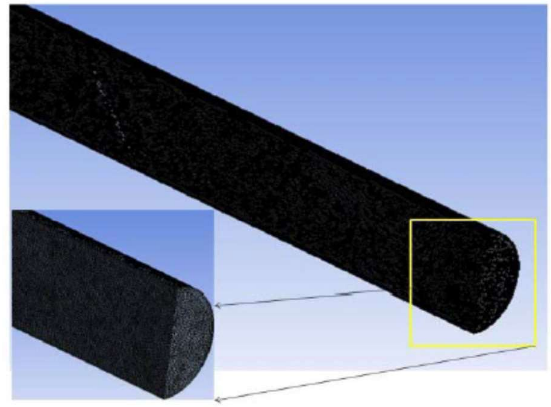

Figure 4. Computational network

The governing equations

Water is selected as the fluid passing the valve. The equations governing the stable flow of Newtonian fluid around the butterfly valve are continuity and momentum relations, which are expressed as follows:

$$\nabla . V = 0 \quad (1)$$

$$\frac{\partial(\rho \bar{u}_i \bar{u}_j)}{\partial x_j} = -\frac{\partial p}{\partial x_i} + \frac{\partial}{\partial x_j}\left[(\mu + \mu_t)\left(\frac{\partial \bar{u}_i}{\partial x_j} + \frac{\partial \bar{u}_j}{\partial x_i}\right)\right] - \frac{2}{3}\frac{\partial(\rho k)}{\partial y} \quad (2)$$

Where

$$\mu_t = \rho c_\mu \frac{k^2}{\varepsilon} \quad (3)$$

This simulation establishes an incompressible flow with viscosity around the butterfly valve disc. The desired flow pattern represents the turbulence of the flow. For this purpose, the ε-k turbulence model is used to simulate the turbulence flow. This turbulence model does not have the nonlinear damping functions required in other turbulence models and therefore has more accuracy and needs less solving time [10]. K-Ɛ model uses the following transfer equation to simulate the flow:

$$\frac{\partial}{\partial x_j}(\rho k \bar{u}_j) = \frac{\partial}{\partial x_j}\left[\left(\mu + \frac{\mu_t}{\delta_t}\right)\frac{\partial k}{\partial x_j}\right] + \mu_t\left[\frac{\partial \bar{u}_i}{\partial x_j} + \frac{\partial \bar{u}_j}{\partial x_i}\right]\frac{\partial u_i}{\partial x_j} - \rho\varepsilon \quad (4)$$

$$\frac{\partial}{\partial x_j}(\rho \varepsilon \bar{u}_j) = \frac{\partial}{\partial x_j}\left[\left(\mu + \frac{\mu_t}{\delta_t}\right)\frac{\partial \varepsilon}{\partial x_j}\right] + c_{\varepsilon 1}\mu_t\left[\frac{\partial \bar{u}_i}{\partial x_j} + \frac{\partial \bar{u}_j}{\partial x_i}\right]\frac{\partial u_i}{\partial x_j}\frac{\varepsilon}{k} - \rho c_{\varepsilon 2} \quad (5)$$

In the wall, kwall and εwall values are zero. In this stable flow, the physical properties and flow conditions used to solve the flow equations are shown in Table 1.
The segregated flow model solves the flow equations. A corrective prediction approach obtains the relationship between momentum equations and continuity in a segregated method. Before performing the simulation, the initial conditions must be set over the entire flow range. The measured pressure is set to zero, while the turbulent dissipation rate, chaotic kinetic energy, and velocity equal the initial flow values. The initial values for the flow field simulations are shown in Table 1.

Table 1 - Values of parameters and constants used in the simulation

Variable	Value
Fluid density	998 kg/m3
Fluid viscosity	0.001003 kg/m.s
Inlet velocity	1, 2, 3 m/s
Solver model	Symmetrical and stable
Flow type	Turbulence (K-E model)
Working pressure	101.3 kPa

Functional characteristics of the valve

The description of a butterfly valve usually includes the evaluation of the most common performance factors such as pressure drop, hydrodynamic torque, flow coefficient, drop coefficient, and hydrodynamic torque coefficient [11]. Pressure drop on a valve is often attributed to flow disorders such as blockage, flow separation, and mixing. The pressure drop depends on the disc angle configuration and the flow rate for butterfly valves. The pressure drop is shown in equation 6 by the absolute pressure differential between the upstream measured pressure and the downstream measured pressure.

$$\Delta P_{\theta} = | P_{u\theta} - P_{d\theta} \quad (6)$$

The pressure drop decreases with increasing valve opening angle for a specific flow rate due to less flow interference. In accordance with [11], we measured upstream and downstream pressures at intervals of twice the valve diameter and six times the diameter of the valve, respectively. The coefficient of flow and hydrodynamic torque are the main factors concerning the selection and evaluation of valves. These two coefficients are used to ensure proper valve performance in the piping system. The flow coefficient is proposed to relate the pressure drop across the valve to its discharge at the desired opening angle. The appropriate valve size is determined for many applications by the flow coefficient. The main relation for estimating the flow coefficient in the industry is proposed in equation 7.

$$c_v = Q \sqrt{\frac{s_g}{\Delta P}} \quad (7)$$

Where ΔP, which is the pressure difference at intervals, is twice the diameter of the disk upstream and six times the diameter of the disk downstream, Q is the flow rate, and sg is the specific gravity of the fluid, which equals one for water. Hydrodynamic torque is also obtained from the force applied by the fluid hitting the disk wall and creating torque around the shaft. The hydrodynamic torque coefficient is also calculated by Equation 5, where T is the torque applied by the flow and D is the disk's diameter.

$$c_t = \frac{T}{D^3 \Delta P} \quad (8)$$

In addition to the factors mentioned, another factor that affects accuracy is the quality of networking. Theoretically, more elements in the geometry result in higher network quality and greater accuracy in the results, increasing the computation time. Simulation and analysis are performed for networks with different sizes at an opening angle of 60 °, and the hydrodynamic torque coefficient, as shown in figure 5, is calculated to determine the result changes with the number of network elements and select the network with optimal geometry.
According to the ANSYS software [13] and performing simulations using different networking by the software, the optimal network with 325150 cells was used.

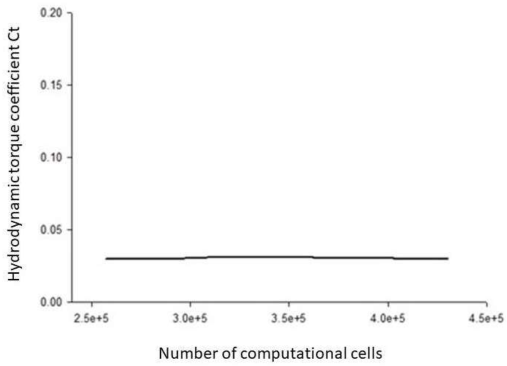

Hydrodynamic torque coefficient	0.0297	0.0297	0.0309	0.0297
Number of cells	256891	289127	325150	430240

Figure 5. Checking the independence of the results from accuracy in the network

Results

A common feature of the simulated flow at all opening angles is the creation and eventual loss of a pair of rotating vortices that form after passing around the butterfly valve. The flow lines along the valve are separated from the disk plate and cause a lot of turbulence and rotation [12].

Figure 6 shows the flow lines around the butterfly valve at an opening angle of 45˚ and a flow velocity of 3 m/s. As can be seen, vortices are formed downstream of the valve, and flow separation is also observed. The formation of vortices downstream is a phenomenon that can be observed at all velocities and opening angles except in the fully open state.

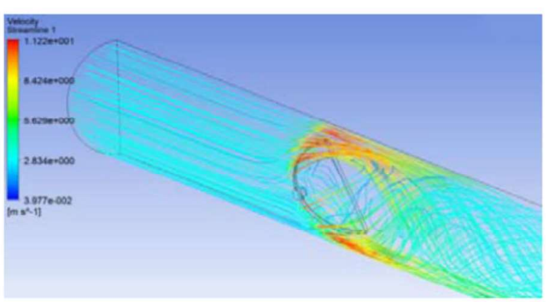

Figure 6. Flow lines around the disk at a velocity of 3 s/m and an angle of 45˚

Figure 7 shows the velocity contours on the center plate of the valve at different opening angles. The velocity is three m/s. As can be seen, the flow is uniform in the fully open state, and no separation of the flow is observed. The flow around the disk is disturbed by increasing the opening angle, and the extent of separation increases. The occurrence of separation downstream and the formation of vortices are associated with a sudden drop in pressure in the valve, and they increase with increasing opening angle. Increasing the angle reduces the area between the edge of the disc and the tube wall and increases the flow rate, which in turn increases the separation of flow from the edge of the disk.

Figure 8 shows the different inlet velocities for the 45° opening angle. It is observed that as the velocity increases, the turbulence area behind the valve disc widens and extends further away from the rear of the disc.

Figure 9 also shows velocity vectors at an opening angle of 75˚ around the disk. As can be seen, the flow around the edge of the disk is highly turbulent, and the vortices behind the disk are larger. The edge of the disc at this angle has a small distance from the wall, reducing the level of flow. Therefore, high-velocity fluid jets form near the edge of the disc.

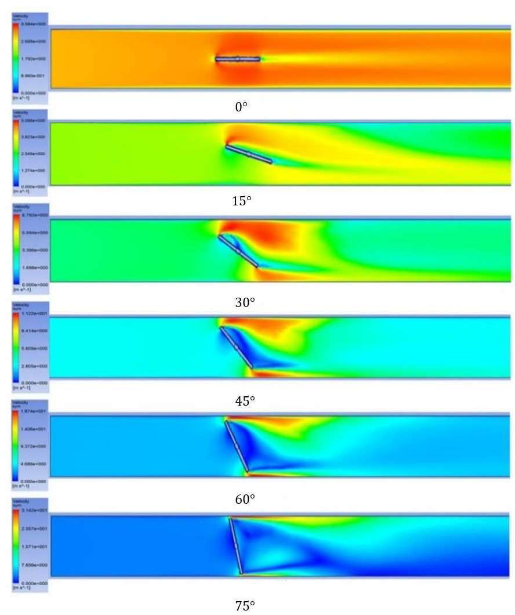

Figure 7. Velocity contours at different angles of disk placement and *inlet velocity* of 3 m/s

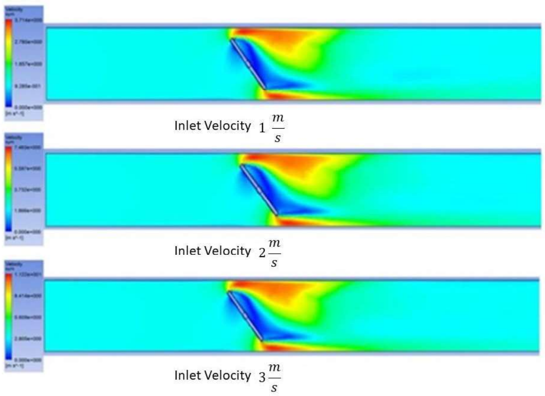

Figure 8. Velocity contours for different *inlet velocities* at an opening angle of 45 $^{\circ}$

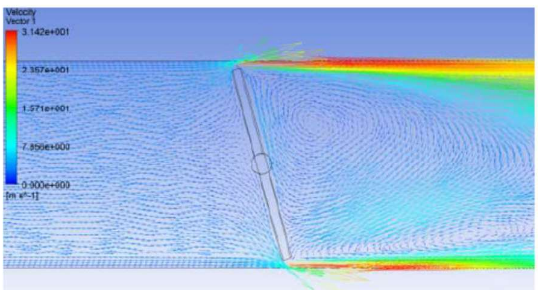

Figure 9. Velocity vector near the disk with an angle of 75°

Figure 10 also shows the pressure distribution in the pipe. It is observed that higher pressure is always formed in front of the disk due to its placement as an obstacle in the flow path. In the areas behind the disk, the pressure values are inverted due to the formation of vortices and turbulent flow. A sharp decrease in pressure at the edge of the disk increases the velocity in this area. After passing through this area and downstream, the velocity decreases, and the pressure increases. The flow is almost uniform when the valve is at a zero-degree opening angle, and no flow separation is observed. As the angle increases to 15°, a slight separation is formed but reattached to the surface. At an angle of 30°, the flow downstream of the disk is completely separated. Similarly, with increasing opening angle, flow separation and reverse pressure have increased in other angles.

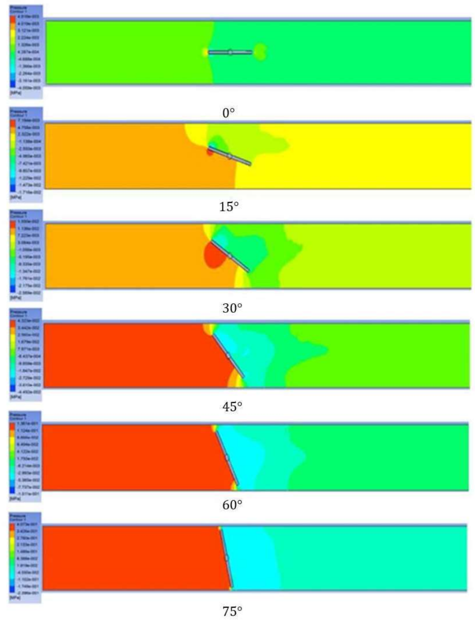

Figure 10. Pressure contours at inlet velocity 3 and different angles

In order to validate the simulation, the results are compared with the experimental values of Chaiworapuek. The model geometry is drawn based on its dimensions. The torque calculated in this study is compared with the experimental results in figure 11. The calculated error in this comparison is 3.1% at the maximum value. The maximum error is calculated at an opening angle of 75°, which is caused by turbulence and the formation of vortices at this angle, and may be due to the inability of the selected turbulence model to simulate this phenomenon near the wall. As expected, with increasing angle and velocity, the applied torque also increases.

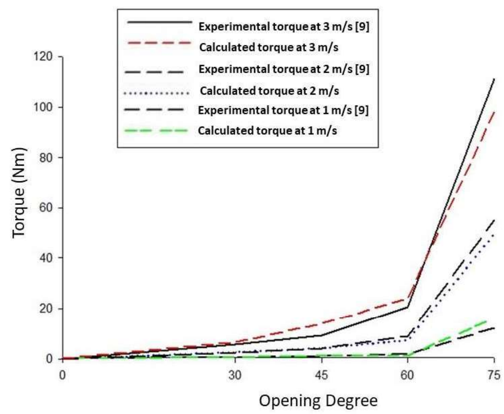

Figure 11. Calculated torque at different velocities and angles compared to experimental results

Figure 12 shows the calculated flow coefficient values. The flow coefficient is negatively correlated with the pressure drop across the valve and decreases with increasing pressure drop at high opening angles. Therefore, it can be said that flow coefficient values decrease with increasing the opening angle.

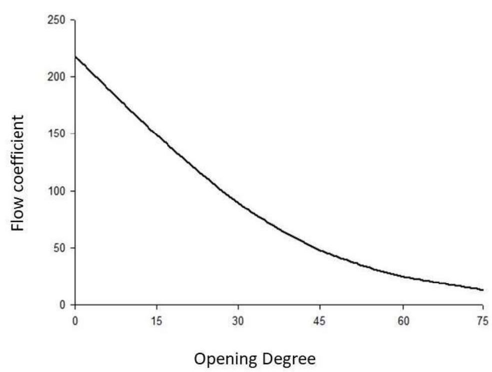

Figure 12. Flow coefficient calculated at different angles and inlet velocity of 3 m/s

Figure 13 also shows the hydrodynamic torque coefficient changes after increasing the size of the opening angle. As can be seen, the maximum torque coefficient occurs at an angle of 15˚. This value is approximately zero at zero opening angle (fully open state).

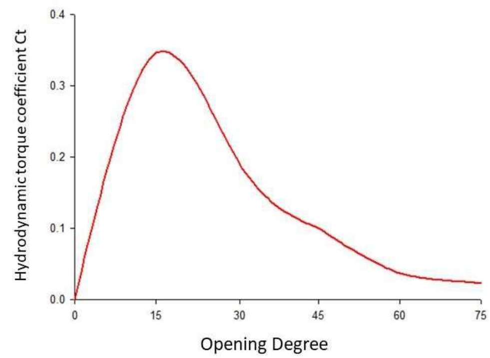

Figure 13. Torque coefficient calculated at different angles and inlet velocity of 3 m/s

Values of pressure drop through the butterfly valve are checked. These values were calculated to find the dimensionless value of the dissipation factor (K). The K values are not independent of the flow rate and are affected by changing the position of the valve disk. As the angle of the valve disc increases, the amount of drop coefficient increases. The results are shown in figure 14. The figure shows that the drop coefficient is independent of the inlet conditions but is directly related to the opening angle of the butterfly valve.

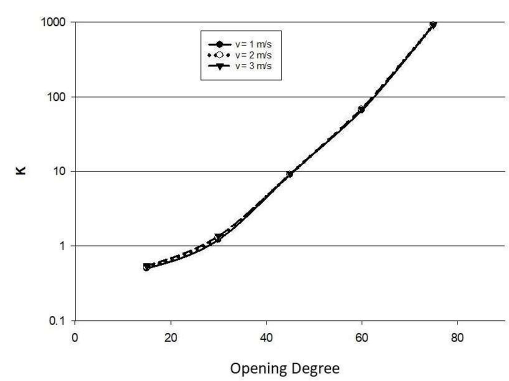

Figure 14. Loss coefficient characteristics at different opening angles for different flow inlets

The torque characteristic used to rotate the butterfly valve disc in 5 positions of the disc valve, consisting of 15˚, 30˚, 45˚, 60˚, and 75˚, has been investigated. The inlet velocity is set to 1, 2, and 3 meters per second. The results are shown in figure 15. As the inlet velocity increases, the torque used to move the disk position gets bigger. Also, the torque increases as the flow area decreases.

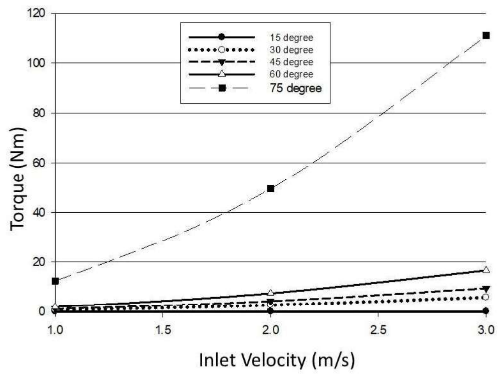

Figure 15. Comparison of torque characteristics for different opening angles and different inlet velocities

Conclusion

Flow characteristics in butterfly valves with different opening angles and incompressible flow regimes have been investigated using ANSYS CFX software. From the obtained results, it was observed that the pressure drop across the valve and the flow coefficient are directly related to the disk placement angle. Therefore, increasing the disk angle leads to an increase in pressure drop and consequently a decrease in flow coefficient. The main advantage of this control valve, which is the minimum pressure drop in the fully open state, was also investigated. According to previous studies, the maximum value of the hydrodynamic torque coefficient is somewhere between the opening angle of 70˚ to 80˚. In our calculations, the maximum value was obtained at an angle of 75˚. Also, when the disk is at high opening angles with less distance between the disk and the wall, the flow is highly turbulent. It is recommended to use other turbulence models to simulate the condition near the wall better. This can improve the simulation results, too.

List of abbreviations

Pressure, Pa	P
Flow coefficient	cv
Discharge, gpm	Q
Pressure drop along the valve	ΔP
Hydrodynamic torque coefficient	ct
Hydrodynamic torque (Nm)	T
Disk diameter (mm)	D
Greek signs Density, kg/m3	ρ
Viscosity, kg/m.s	µ
Turbulence distribution rate	Ɛ
Turbulent kinetic energy, J	K

References

[1] Sarpkaya, T., 1961, “Torque and Cavitation Characteristics of Butterfly Valves”, Journal of Applied Mechanics, 28(4), pp. 511-518.
[2] Morris, M. J. and Dutton, J. C., 1989, “Aerodynamic Torque Characteristics of Butterfly Valves in Compressible Flow”, Journal of Fluids Engineering, 111(4), pp. 392-399
[3] Kimura, T., Tanaka, T., Fujimoto, K., and Ogawa, K., 1995,” Hydrodynamic characteristics of a butterfly valve - Prediction of pressure loss characteristics”, ISA Transactions, 34(4), pp. 319- 326.
[4] Ogawa, K. and Kimura, T., 1995, “Hydrodynamic characteristics of a butterfly valve - Prediction of torquecharacteristics”, ISA Transactions, 34(4), pp. 327-333.
[5] Huang, C. and Kim, R. H., 1996, “Three-Dimensional Analysis of Partially Open Butterfly Valve Flows”, Journal of Fluids Engineering, 118(3), pp. 562-568.
[6] Lin, F. and Schohl, G. A., 2004, “CFD Prediction and Validation of Butterfly Valve Hydrodynamic Forces”, Proceedings of World Water and Environmental Resources Congress, Salt Lake City, USA, pp. 1-8.
[7] Song, X. G. and Park, Y. C., 2007, “Numerical Analysis of Butterfly Valve-Prediction of Flow Coefficient and Hydrodynamic Torque Coefficient”, Proceedings of the World Congress on Engineering and Computer Science, San Francisco, USA, pp. 759-763.
[8] Perma, B., Bahojani, S., and Gopalakrishnan, N., 2010, “Design Optimization of Butterfly Valve Using CFD”, Proceedings of the 37th National & 4th International Conference on Fluid Mechanics and Fluid Power, IIT Madras, Chennai, India.
[9] Chaiworapuek, W., 2007, The Engineering Investigation of the Water Flow past the Butterfly Valve, MS Thesis, Institut National Des Sciences Appliquees De Lyon – France.
[10] B. Mohammadi and O. Pironneau, Analysis of the K-Epsilon Turbulence Model (Research in Applied Mathematics), John Wiley & Sons Ltd (Import) (August 1994).
[11] Bosserman, B.E., Ali, A., Schuraytz, I.M., 2012, Butterfly Valves: Torque, Head Loss, and Cavitation Analysis AWWA Manual; M49, 2nd ed., American Water Works Association, Denver, CO.
[12] Henderson, A.D., Sargison, J.E., Walker, G.J., and Haynes, J.H., 2008, “A Numerical Prediction of the Hydrodynamic Torque Acting on a Safety Butterfly Valve in a Hydro-Electric Power Scheme,” WSEAS Trans. on Fluid Mechanics, 1(3), pp. 218-223.
[13] ANSYS CFX 10.0 User’s Manual, ANSYS, Inc